

Plasmon printing – a new approach to near-field lithography

Pieter G. Kik, Stefan A. Maier, and Harry A. Atwater
Thomas J. Watson Laboratory of Applied Physics, California Institute of Technology,
Pasadena, CA 91125, USA

ABSTRACT

We propose a method for replicating patterns with a resolution well below the diffraction limit, using broad beam illumination and standard photoresist. In particular it is shown that visible exposure ($\lambda=410$ nm) of silver nanoparticles in close proximity to a thin film of g-line resist (AZ 1813) can produce selectively exposed areas with a diameter smaller than $\lambda/20$. The technique relies on the local field enhancement around metal nanostructures when illuminated at the surface plasmon resonance frequency. The method can be extended to various metals, photosensitive layers, and particle shapes.

INTRODUCTION

The continuing size reduction of integrated circuits to nanometer scale dimensions requires the development of new lithographic techniques. It is becoming increasingly difficult and complex to use the established method of optical projection lithography at the short optical wavelengths required to reach the desired feature sizes. For example, the use of wavelengths in the deep ultraviolet,¹ the extreme ultraviolet (EUV),² or the X-ray regime³ requires increasingly difficult adjustments of the lithographic process, including the development of new light sources, photoresists and optics. That this is seen as a major problem in the industry is clear from the large scale efforts to develop alternative approaches to nanolithography.

A relatively established method for the production of high-resolution patterns is the use of focused particle beams, e.g. a focused electron beams⁴ or ion beams,⁵ that expose a resist layer as it is scanned across the substrate. Although this produces high-resolution patterns, the sequential nature of the technique results in long writing times. Other sequential techniques involve the use of a local probe such as the tip of an Atomic Force Microscope (AFM)⁶ or the tip of a Near-field Scanning Optical Microscope (NSOM).⁷ Two parallel approaches to nanolithography that do not require short-wavelength light are micro-contact printing,⁸ evanescent near field lithography (ENFOL)^{9,10} and evanescent interferometric lithography (EIL).¹¹ The latter two methods employ the evanescent optical field set up directly below a contact mask for exposure, and promise a resolution as high as $\lambda/20$.¹²

In this article we propose a new approach to nanolithography that can potentially produce sub-wavelength structures using broad beam illumination of standard photoresist with visible light. The technique is related to ENFOL, but in addition it uses resonant local field enhancement to obtain sub-wavelength resolution. The method is based on the plasmon resonance occurring in nanoscale metallic structures. When a metal nanoparticle is placed in an optical field, it exhibits a collective electron motion known as the surface plasmon oscillation. When the diameter of the particle is much smaller than the applied wavelength, the charge movement produces an oscillating dipole field. This can result in strongly enhanced electrical fields near the particle when the excitation occurs at the resonance frequency. For a spherical particle, the plasmon

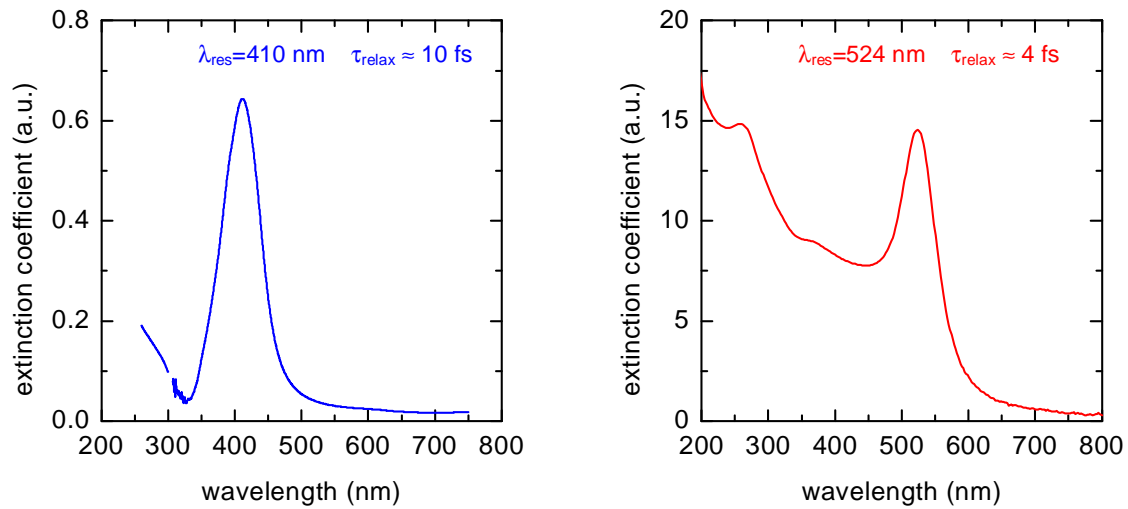


Figure 1: Extinction measurements of colloidal suspensions of (a) Ag nanoparticles (diameter 41 nm) and (b) gold nanoparticles (diameter 30 nm) in water, showing enhanced absorption and scattering at the surface plasmon resonance frequency.

resonance occurs at the wavelength λ for which $\epsilon_{\text{particle}}(\lambda) = -2 \times \epsilon_{\text{matrix}}(\lambda)$ with ϵ the dielectric function of the particle and the surrounding material respectively. The magnitude of the field enhancement depends strongly on the carrier relaxation time in the nanoparticle. Metals with long relaxation times such as gold ($\tau_{\text{relax}} \approx 4 \text{ fs}$) and silver ($\tau_{\text{relax}} \approx 10 \text{ fs}$) show strong resonances in the visible and near-UV range.

The occurrence of the plasmon resonance can be clearly observed in extinction measurements. Figure 1(a) shows the extinction of an aqueous solution of Ag nanoparticles. A strong increase in the extinction is observed around 410 nm. This high extinction is the result of a strongly enhanced absorption and scattering. The resonantly excited electron oscillation induces enhanced resistive heating, while the oscillating dipole inside the particle generates dipole radiation adding to the total extinction. Figure 1(b) shows the extinction of a suspension of 30 nm diameter Au particles in water. This system also shows a plasmon resonance ($\lambda_{\text{res}} = 524 \text{ nm}$), but additionally an absorption band is observed at shorter wavelengths. This absorption is the result of interband transitions in the gold nanoparticles, and does not contribute to the coherent plasmon oscillation.

As shown above, illumination of metal nanoparticles at the plasmon resonance produces

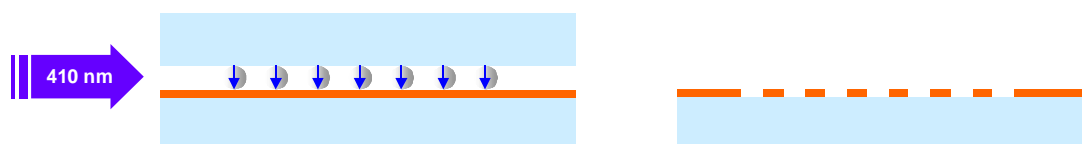


Figure 2: Schematic representation of plasmon printing, showing (a) glancing angle illumination of using polarized visible light, producing enhanced resist exposure directly below the metal nanostructures on the mask layer, and (b) the resulting pattern in the resist layer after development.

a strongly enhanced dipole field near the particle. This enhanced field can be used to locally expose a thin layer of resist. A schematic of the printing process is shown in Fig. 2. In order to obtain intensity enhancement directly below the particle, the incoming light should be polarized approximately normal to the resist layer (p-polarization), implying the need for glancing incidence exposure. We propose to call this approach “plasmon printing” because of its parallel nature and the use of surface plasmons for exposure. Plasmon printing could enable the generation of sub-wavelength printed replicas of nanoscale structures in a parallel fashion, using standard photoresist and broad beam illumination in the visible.

SIMULATIONS

The applicability of the proposed scheme depends on the magnitude of the field enhancement effect, and the time-dependent field distribution around the metal nanoparticles. Field distributions during illumination were determined using 3D Finite Difference Time Domain (FDTD) calculations. The simulated geometry consists of a 40 nm diameter spherical particle on a 25 nm thick resist layer on glass. The surrounding medium is taken to have $n=1$ (air or vacuum). The simulations involved 10^6 mesh points in a graded mesh density to obtain a high mesh density (2.2 nm cells) around the metal particle while keeping the total number of mesh lines manageable. Glancing angle illumination was simulated by a plane wave propagating in the +x direction. The wave was polarized in the z-direction to obtain maximum field enhancement above and below the particle. The simulation parameters are listed in Table I. The behavior of the particles was simulated using a Drude model with the dielectric function given by

$$\epsilon_{metal}(f) = 1 - \left(\frac{f_p}{f} \right)^2 \quad (1)$$

with f_p the bulk plasma frequency. The values for f_p in Table I were chosen to yield the correct surface plasmon resonance frequency as measured for nanoparticles in water as observed in Fig.

	Ag	Au
Diameter (nm)	40	40
f_{plasma}	1.47×10^{15}	1.08×10^{15}
f_{relax}	10^{14}	2.5×10^{14}
f_{exc}	7.32×10^{14}	5.59×10^{14}
λ_{exc}	410 nm	537 nm
$\epsilon_{\text{glass}}(\lambda_{\text{exc}}) (n)$	2.25 (1.5)	2.25 (1.5)
$\epsilon_{\text{resist}}(n)$	2.91 (1.71)	2.76 (1.66)
ϵ_{air}	1	1
#steps	10000	5000
Δt	2.73×10^{-18}	3.58×10^{-18}
t_{end}	2.73×10^{-14}	1.79×10^{-14}
Optical cycles	20	10

Table I: Parameters used in the 3D Finite Difference Time Domain Calculations.



Figure 3. Snapshots of E_z^2 obtained by 3D Finite Difference Time Domain simulations using the parameters listed in Table I, showing (a) the case of a 40 nm diameter silver particle and (b) a 40 nm diameter gold particle on a 25 nm thick resist layer on glass under glancing angle illumination with p-polarized light. In both cases enhanced exposure is observed in an area with a diameter $d < 0.05\lambda$.

1. The total length of the simulation was set to several times the relaxation time to approach the steady state amplitude of the field oscillation in and around the particles. It should be noted that the effect of resist absorption on the plasmon resonance has not been taken into account in these calculations. In the case of a highly absorbing resist layer, this may reduce the magnitude of the field enhancement.

The incoming wave is p-polarized, and consequently the main contribution to the total field strength directly beneath the particle is E_z . Figure 3(a) shows a snapshot of E_z^2 around a 40 nm silver particle near the end of the simulation. The image shows two fronts of high field to the left and right of the particle showing as broad dim features, and a strong opposing field inside the particle in an area where the external field is zero. This is the result of the 90° phase lag between exciting field and induced field associated with resonant excitation. Note that while the particle is excited at 410 nm, the area of enhanced exposure is only ~ 20 nm in diameter. This suggests that in this type of geometry, it is possible to print features as small as $\lambda/20$. Since the field strength drops off gradually (but rapidly) with distance, the size of the exposed area will depend on the intensity and the duration of the exposure. Figure 3(b) shows E_z^2 around a 40 nm gold particle near the end of the simulation. The region of enhanced exposure is smaller than in the case of silver, indicating a lower exposure contrast between patterned and unpatterned areas. The calculations shown in Fig. 3 indicate that the minimum feature size most likely will be limited by practical issues such as fluctuations in intensity or mask-to-sample distance.

EXPERIMENTS

Our initial experiments were aimed at obtaining a proof-of-principle. To avoid difficulties in achieving the desired nanoscale spacing between mask and resist layer, instead of using a conventional mask our experiments involve 41 nm diameter silver nanoparticles (the “mask”) spray-deposited onto a thin resist layer. Glass substrates (surface roughness $< 5 \text{ \AA}$ RMS) were coated with standard g-line resist (AZ1813, Shipley), which has its maximum sensitivity in the wavelength range 300–450 nm. The resist was diluted with AZ EBR dilutant (ratio AZ1813:EBR = 1:4) and subsequently spin coated onto the substrates at 5000 rpm (60s) producing a smooth ~ 75 nm thick film. The smoothness is important since in the experiments ~ 40 nm diameter

features need to be resolved. For illumination the output of a 1000 W Xe arc lamp was sent through a monochromator set to a wavelength of 410 nm, and subsequently passed through a polarizer to obtain polarization normal to the sample surface. The beam was vertically compressed using a cylindrical lens to increase the power density, and sent to the sample at glancing incidence. A photograph and a sketch of the illumination setup are shown in Fig. 4. The sample was suspended to prevent exposure by light scattered from the sample holder, see Fig. 4(b). The applied power densities were of the order of $1 \text{ mW}/\text{cm}^2$, and exposures times were in the range 10s – 300s. After exposure the films were developed for 20s in developer (MF317), mixed with water in a 1:1 ratio to slow down development. Conventional exposure of the 75 nm thick resist layers showed normal development at these development conditions. The developed films were investigated using contact mode Atomic Force Microscopy.

The developed films were found to still have some residual nanoparticles on the surface. Using the AFM tip it was possible to move the particles over the surface, producing streaks in the AFM images. In addition to the particles, nanoscale dips were observed in the resist film, suggesting enhanced exposure in sub-wavelength size areas. Figure 5(a) shows an AFM scan of a $300 \times 300 \mu\text{m}$ area, showing an approximately circular depression in the resist layer. Figure 5(b) shows a cross-section through the depression, showing a lateral size of approximately 50 nm, and a depth of 12 nm, possibly limited by the AFM tip shape. It should be noted that the identification of these nanoscale imprints is not fully unambiguous due to the relatively large resist roughness after development. Experiments are underway to further investigate the effect of plasmon enhanced resist exposure.

The calculations and experiments presented here dealt exclusively with isolated 30-40nm diameter metal particles. When larger particles are used, the field enhancement will eventually drop due to the excitation of multipolar oscillations in the particles. Going to smaller particles, carrier relaxation due to surface scattering will eventually start to dominate the relaxation time, adversely affecting the field enhancement. Further experiments should focus on the effect of

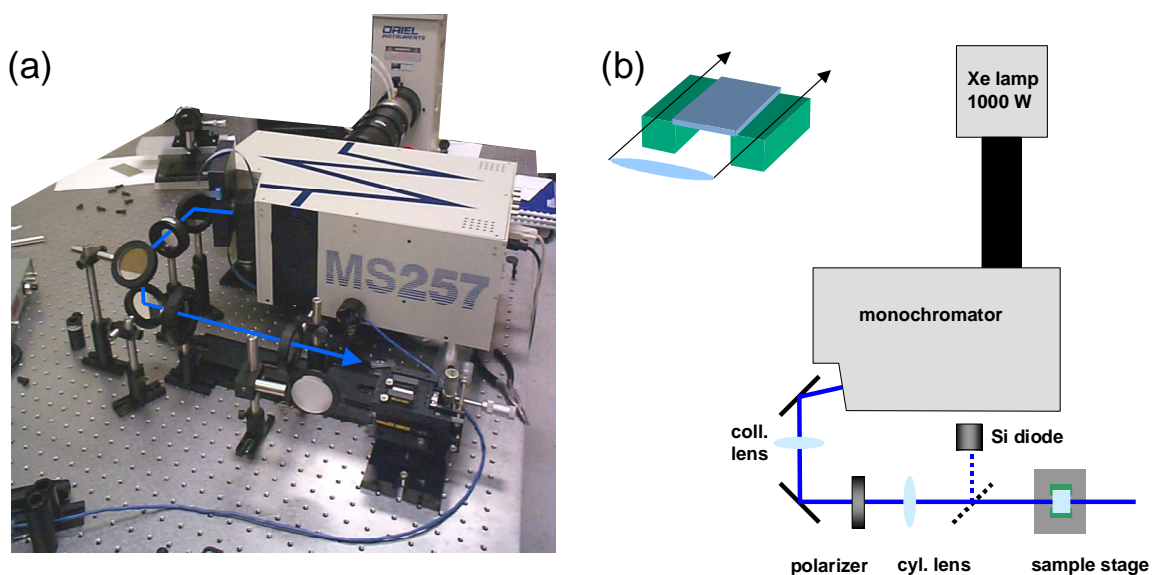


Figure 4: (a) Photograph and (b) schematic representation of the illumination setup. An enlarged schematic of the sample holder is included, showing the approximate beam size. The beam direction is indicated by the arrows.

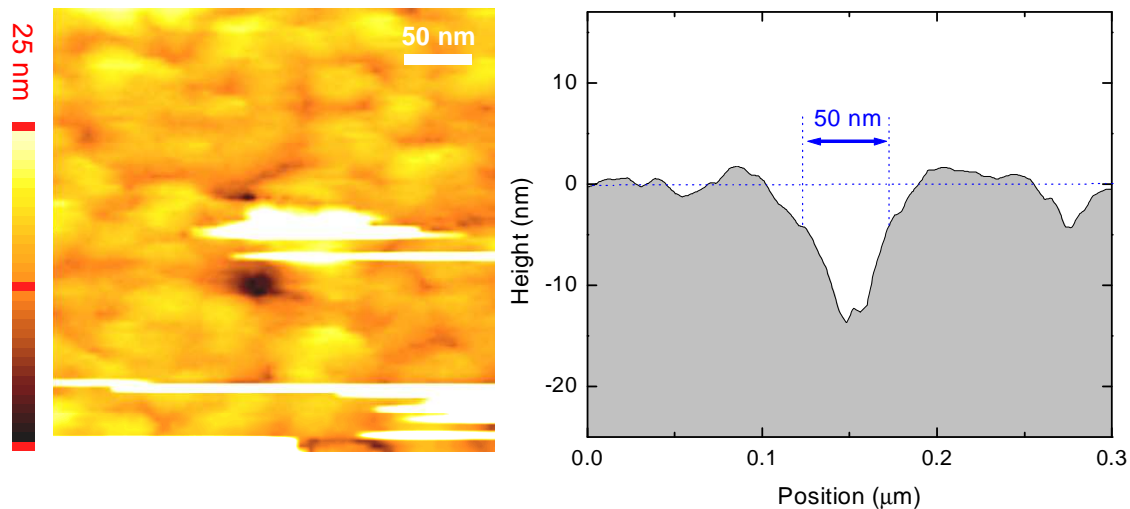


Figure 5: (a) Atomic Force Microscopy image of a 75 nm thick exposed and developed AZ1813 resist layer, showing the presence 41 nm Ag particles on the surface (streaks) and a nanoscale depression attributed to locally enhanced resist exposure below a nanoparticle due to resonant excitation of a surface plasmon oscillation in the particle. (b) A cross-section through the imprint, showing a feature size of 50nm (0.1λ).

particle-particle interactions in more complex patterns, the effect of the angle of incidence on exposure, and the effect of particle shape on the field enhancement.

CONCLUSIONS

We have shown that the local field enhancement occurring around metal nanoparticles when they are excited at the surface plasmon resonance frequency can be used to print nanoscale features in thin resist layers. Feature sizes below $\lambda/10$ can be generated using visible illumination and standard g-line photoresist.

REFERENCES

- ¹ M. Rothschild, T. M. Bloomstein, J. E. Curtin, D. K. Downs, T. H. Fedynyshyn, D. E. Hardy, R. R. Kunz, V. Liberman, J. H. C. Sedlacek, R. S. Uttaro, A. K. Bates, and C. Van Peski, *J. Vac. Sci. Technol. B* **17**, 3262 (1999)
- ² C. W. Gwyn, R. Stulen, D. Sweeney, and D. Attwood, *J. Vac. Sci. Technol. B* **16**, 3142 (1998)
- ³ J. P. Silverman, *J. Vac. Sci. Technol. B* **16**, 3137 (1998)
- ⁴ M. A. McCord, *J. Vac. Sci. Technol. B* **15**, 2125 (1997)
- ⁵ J. Melngailis, *Nucl. Instr. & Meth. B* **80**, 1271 (1993)
- ⁶ M.A. McCord and R. F. W. Pease, *J. Vac. Sci. Technol. B* **1**, 86 (1986)
- ⁷ E. Betzig and J. K. Trautman, *Science* **257**, 189 (1992)
- ⁸ X. M. Zhao, Y. N. Xia, and G. M. Whitesides, *J. Mat. Chem.* **7**, 1069 (1997)
- ⁹ M. M. Alkaisi, R. J. Blaikie, S. J. McNab, R. Cheung, and D. R. S. Cumming, *Appl. Phys. Lett.* **75**, 3560 (1999)
- ¹⁰ J. G. Goodberlet, *Appl. Phys. Lett.* **76**, 667 (2000)
- ¹¹ R. J. Blaikie, and S. McNab, *Appl. Opt.* **40**, 1692 (2001)
- ¹² S. J. McNab, and R. J. Blaikie, *Appl. Opt.* **39**, 20 (2000)